Journal of Magnetism and Magnetic Materials 324 (2012) 1601–1605

Contents lists available at SciVerse ScienceDirect

Journal of Magnetism and Magnetic Materials

journal homepage: www.elsevier.com/locate/jmmm

Hysteretic giant magnetoimpedance effect analyzed by first-order reversal curves

F. Béron [a,*], L.A. Valenzuela [a], M. Knobel [a], L.G.C. Melo [b], K.R. Pirota [a]

[a] Instituto de Física Gleb Wataghin, Universidade Estadual de Campinas, 13083-859 Campinas (SP), Brazil
[b] Department of Telecommunication and Robotics Engineering, Universidade Federal de São João del-Rei, 36420-000 Ouro Branco (MG), Brazil

ARTICLE INFO

Article history:
Received 14 October 2011
Received in revised form
24 November 2011
Available online 9 December 2011

Keywords:
Giant magnetoimpedance (GMI)
First-order reversal curve (FORC)
Amorphous ribbons
Hysteron

ABSTRACT

We applied the first-order reversal curve method to hysteretic giant magnetoimpedance (GMI) of soft magnetic amorphous ribbons with a well-defined transversal domain structure and quasi-anhysteretic magnetization behavior. In opposition to major curve, it gives access to the distribution of local irreversible changes of the transverse permeability, which undergo a gradual transition. Results show that hysteretic GMI effect consists of three distinct regimes depending on the applied field. An interlinked hysteron/anti-hysteron model is proposed to analyze the obtained results, which allows one to follow the influence of frequency and anisotropy upon the irreversible switches probed by GMI.

1. Introduction

The giant magnetoimpedance (GMI) effect consists of a drastic change (up to hundreds of percent) of the electrical impedance Z of a magnetically soft conductor upon application of an external magnetic field H. It is related to variations of the effective magnetic permeability μ, which is strongly affected by the external magnetic field and the frequency f of the ac driving current i. In magnetic metals, the variation of μ as a function of H and f governs the change of the penetration depth δ of the electromagnetic fields through the sample, producing the GMI effect. Although it was first observed around seven decades ago [1], its intense investigation started only in 1994 [2]. This "rediscovery" of GMI in amorphous soft magnetic alloys attracted much attention of scientific community owing to its potential application in ultra-sensitive magnetic sensors and reading heads, as well as an investigation tool for material parameters [3]. While theoretical models of the transverse permeability μ_t adequately explain the GMI behavior in a broad range of H and f [4–6], improvements have been done to include unsaturated behavior (H less than the anisotropy field H_k) [7]. One notable example is the hysteretic behavior of the GMI curve, which has been observed in several types of systems, mainly ribbons [8–11] and microwires [9,12,13] with transverse or circumferential anisotropy and for relatively low frequencies (tens of MHz and below). It was attributed to various physical phenomenon, predominantly irreversible domain wall motion and axial magnetization switches. This effect is of high technological relevance, especially for applications of GMI at low fields [14]. The hysteresis can be detrimental for applications such as magnetic sensors, while others can take advantage of it, such as memories. However, the previous studies on the subject were limited to GMI and magnetization major curves, which represent the whole system global behavior.

On the other hand, the first-order reversal curve (FORC) method is one of the most powerful tools to investigate the origins and to characterize the materials general hysteretic behavior [15]. Since 1985 it has been successfully applied to probe the magnetization (M) hysteresis in several systems [16–19], but its mathematical nature allows a more general use [15]. The FORC method has already been successfully used to investigate the hysteretic behavior of other parameters: ferroelectricity [20], pressure [21] and giant magnetoresistance (GMR) [22]. The main advantage over major hysteresis curves is that it gives the distribution of local properties, instead of average, which can be crucial when dealing with non-uniform systems. Thereby, the FORC method must be seen as a powerful experimental tool that can be used to probe the hysteretic behavior of any system that respects the wipe-out and congruency conditions [15].

In this article, the measurement procedure of the FORC method was applied to the electrical impedance response as a function of the longitudinal external field of FeCoSiB amorphous ribbons with well-defined transversal domain structure. While their GMI responses exhibit hysteresis at low field, the magnetization presents a quasi-reversible behavior. The FORC results represent the distribution of each local irreversible switch, thereby dissecting the GMI hysteresis. We conceived a new type of hysteron to adapt the traditional FORC analysis to the particular type of hysteresis

* Corresponding author. Tel.: +55 (19) 3521 5504; fax: +55 (19) 3521 4147.
E-mail address: fberon@ifi.unicamp.br (F. Béron).

0304-8853
doi:10.1016/j.jmmm.2011.12.013

exhibited by the GMI signal, which describes an even function. This new analysis is thought to be easily adaptable to similar functions, like magnetoresistance and magnetostriction, among others. The novel established FORC procedure for GMI signal (called GMI-FORC) allows the investigation of the effects of different parameters (current amplitude and frequency, ribbon characteristics, etc.) on the hysteretic process, and so their specific repercussions on the ribbon magnetic structure.

2. Ribbons characterization

Amorphous ribbons of $(Fe_xCo_{1-x})_{70}Si_{12}B_{18}$ (x=0.045–0.050), 22 μm thick, were prepared by melt spinning technique. A proper annealing treatment, described in [23], induced magnetostriction, which constant depends on the Fe/Co ratio. It results of a rather well-defined uniaxial anisotropy with easy axis perpendicular to the ribbon axis, as confirmed by a representative magnetic optical Kerr effect (MOKE) image (Fig. 1). The major magnetization curve as a function of a longitudinal applied field, measured with a high-precision AC induction magnetometer [24], shows a mostly reversible behavior, with a small detectable hysteresis, as expected owing to the transversal anisotropy (Fig. 2).

In contrast, the GMI curve (i=1 mA, f=500 kHz, $\delta \approx 3$ μm) as a function of the longitudinal static applied field reveals a different behavior. In addition to the two typical peaks associated with the anisotropy field clearly visible around $H=\pm 6$ Oe, it exhibits an important hysteretic region at low field ($H=\pm 4.5$ Oe), which is symmetric around the origin (Fig. 2). Magnetization detects longitudinal irreversibility while GMI probes the irreversibility of the transverse permeability μ_t. The combination of both may lead to better understand the local mechanisms governing the magnetization of soft magnetic amorphous ribbons.

3. FORC method

The FORC method is based on the classical Preisach model. The global behavior of the hysteresis is associated with a collection of single square irreversible curves, called mathematical hysterons and representing the hysteresis operators [15]. The method consists of the measurement of increasing minor hysteresis curves starting from different input values, called reversal points (H_r for field-driven hysteresis), and reaching the positive saturation. The mathematical hysterons distribution, the so-called FORC distribution function, $\rho(H, H_r)$, is obtained through the calculation of a second-order mixed derivative of the output variable with respect to the reversal and measuring field values [15]. In the present case, the impedance, which is the output variable, was separated into its real (R) and imaginary (X) parts before the calculation, leading to two distinct FORC distributions (for $H > H_r$):

$$\rho_R(H,H_r) = -\frac{1}{2}\frac{\partial^2 R(H,H_r)}{\partial H \partial H_r} \quad (1)$$

$$\rho_X(H,H_r) = -\frac{1}{2}\frac{\partial^2 X(H,H_r)}{\partial H \partial H_r} \quad (2)$$

Compared to the major hysteresis curve, which gives the average behavior of the hysteretic operators, it presents the advantage to yield the function distribution of those. For complex systems, hysteretic phenomena can not be directly modeled as mathematical hysterons. In such cases, an essential step consists of modeling an assembly of mathematical hysterons that adequately describes the behavior of each hysteretic process occurring [25]. For GMI-FORC, we elaborated a dual-hysteron model that represents the elementary irreversible behavior of the GMI (see Section 4.2). For further interpretation of the FORC diagram, one needs to correctly identify the physical meaning of those dual-hysterons.

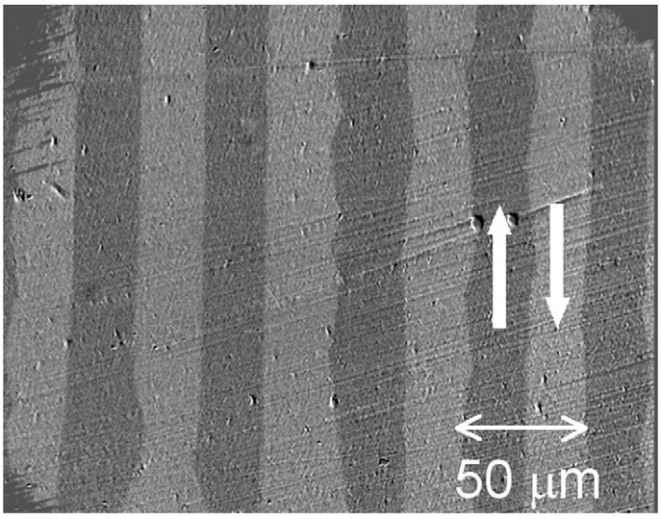

Fig. 1. Top-view MOKE image of the studied FeCoSiB ribbon. The alternation of dark and clear domains signifies antiparallel perpendicular domains, resulting of the well-defined transversal magnetic anisotropy. The arrows indicate the magnetization direction.

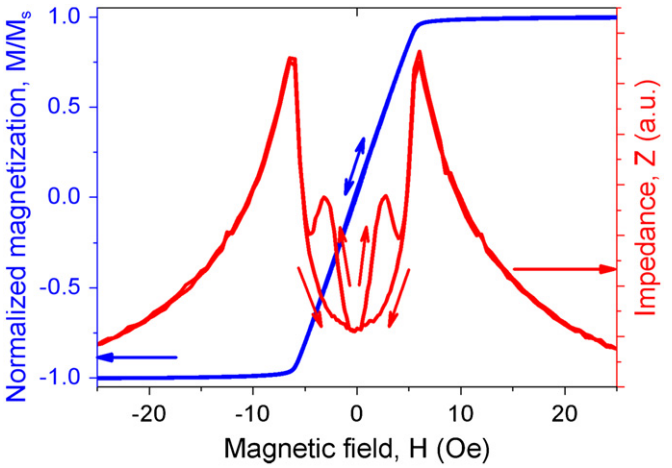

Fig. 2. FeCoSiB ribbon (x=0.045) typical major curves of magnetization and GMI signal (f=500 kHz, i=1 mA, $\delta \approx 3$ μm) under a longitudinal applied field.

4. GMI-FORC

4.1. FORCs

The measured FORC curves (GMI-FORCs) were obtained by measuring the impedance, at a fixed frequency, when H was varied from H_r back to positive saturation (Fig. 3(a), thin colored lines). They were confined in this region, because the reversible behavior occurring at higher field yields a null FORC distribution. In order to avoid artifacts on the FORC distribution and visualize better the irreversible variations, we subtracted the lowest major curve (Fig. 3(a), thick black line) from each FORCs before the FORC distribution calculation.

The resulting FORCs (Fig. 3(b), thin colored lines) are not confined within the two paths described by the major curve, passing through the two hysteretic areas as well as outside them. Therefore, the μ_t irreversibility of the entire ribbon is not constituted of only

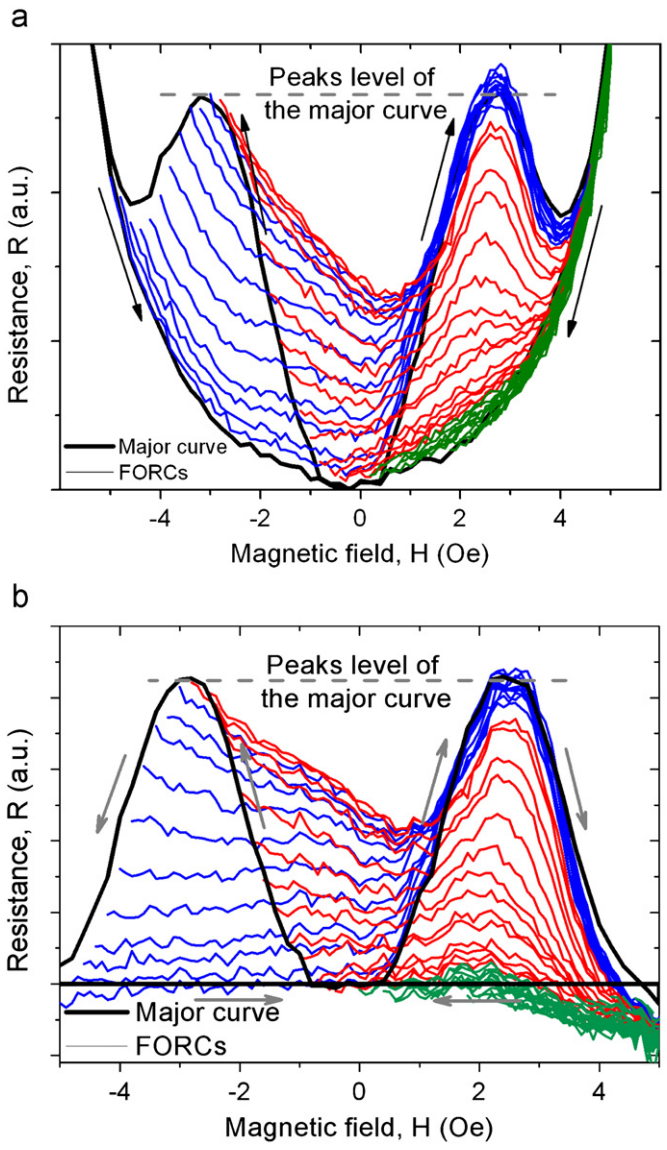

Fig. 3. Low field region of typical major curve (black thick line) and FORCs (thin colored lines, separated into three groups according to their behavior) of the real part of the GMI signal ($x=0.045$, $f=500$ kHz, $i=1$ mA, $\delta \approx 3$ μm). The reversal field step (ΔH_r) and field step (ΔH) were respectively taken as 0.2 and 0.1 Oe, while 100 Oe was applied to completely saturate the ribbon between each FORC. (a) As measured (b) after subtraction of the lowest major curve.

two states, but of several distinct states. This agrees well with a model where local structures, like domains or domain walls, can undergo irreversible change between two values of μ_t. If they were all switching state simultaneously (all together), only the two major curve paths would be accessible. Therefore, the GMI-FORCs clearly indicate a progressive variation of μ_t throughout the whole ribbon, which can be probed due to the particular FORC measurement.

The different FORCs behaviors can be divided into three groups (Fig. 3(b)). FORCs initiating roughly below the left peak ($H_r < -2.7$ Oe, blue lines) remain parallel to each other until joining themselves during the right rise and clearly follow the same path when decreasing afterwards. Interestingly, they move out of the major curve path around the right peak, where they reach higher GMI signal. It may indicate that only a certain proportion of the local structures that can undergo irreversible μ_t transition experiences it, i.e. more transitions occur when performing a FORC that when passing from one saturation field to the other. The next FORCs (until $H_r=0$ Oe, red lines) present a constant behavior (no transition) followed by gradual decrease until remaining completely constant ($H_r > 0$ Oe, green lines). The lack of transition in this region, which yields to a null FORC distribution, reveals that irreversible μ_t change initiates only after inverting the applied field.

On Fig. 3(b), one can see that the FORCs initiating with a negative reversal field (blue and red lines) exhibit an almost flat behavior until $H=0$ Oe. This lack of notable variation is attributed to purely reversible evolution of the transverse permeability between $H=H_r$ and 0 Oe, i.e. absence of irreversible transition. Therefore, in this case, remanent GMI signal variation can be used as a probe of the evolution of the μ_t progressive irreversible transition in the ribbon when sweeping the applied field from one saturation state to the other. The behavior of $R_{H=0\ \mathrm{Oe}}$ suggests that two transitions are occurring: the system first passes from low μ_t states to high μ_t states when H decreases until -2.7 Oe, where a return to low μ_t states is observed, reaching the same level as before the transition ($H=0$ Oe) (Fig. 4). It is worth noting that the maximum does not correspond with the GMI peak position on the as-measured major curve (± 3.2 Oe), but concord after subtraction of the lowest major curve. This shift is therefore attributed to the presence of reversible contribution.

4.2. Dual-hysteron model

Based on the FORCs analysis, the complex irreversible behavior of the GMI signal requires more than one simple bistable hysteron to be adequately modeled [25]. The behavior of the first FORCs regime ($H_r < -2.7$ Oe) is adequately represented by a conventional hysteron. A down transition occurs at a negative H_r ($H_{\downarrow}^{-}$) which returns at the high μ_t state, $\mu_{\uparrow}$,for a positive applied field ($H_{\uparrow}^{+}$) (Fig. 5). This process is expected to produce a positive peak on the FORC distribution ($\rho > 0$). On the other hand, the following FORCs regime (-2.7 Oe $< H_r < 0$ Oe) suggests an inverse process: an up transition takes place at a negative H_r ($H_{\uparrow}^{-}$) therefore followed by a down one for a positive applied field ($H_{\downarrow}^{+}$). We called anti-hysteron this mirror image of a conventional hysteron, because it yields to an anti-peak in the FORC distribution, i.e. $\rho < 0$. The switch between those two operators is possible only through their common upper level. By example, an exchange from the hysteron path to the anti-hysteron one occurs if, after the hysteron $H_{\uparrow}^{+}$ transition, the field increases until the anti-hysteron

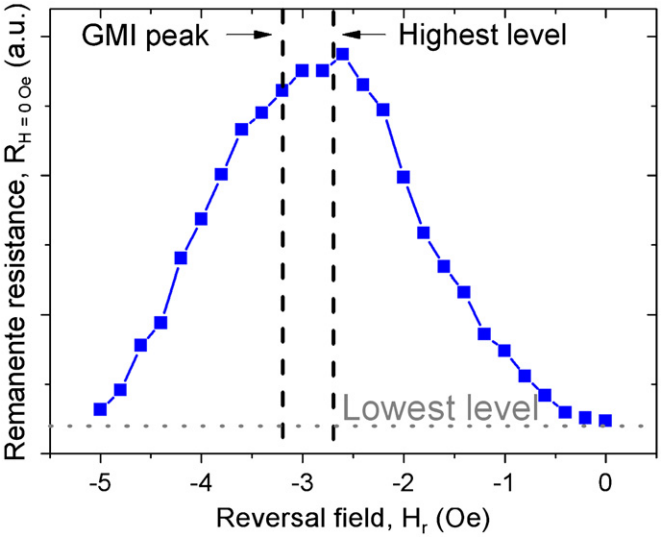

Fig. 4. Remanent real part of the GMI signal as a function of the reversal field values. The vertical dashed lines indicated the position of the GMI major curve peak and the maximum, while the horizontal dotted line shows the minimum level.

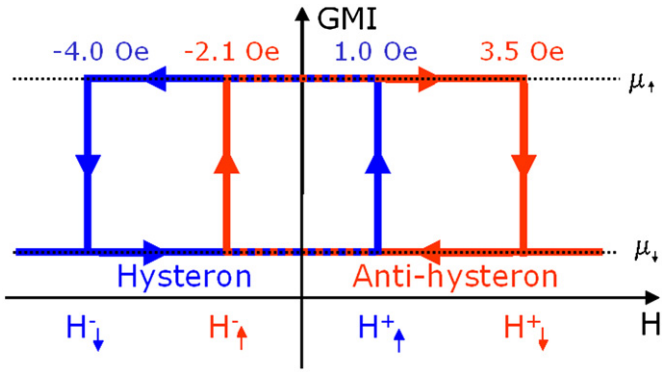

Fig. 5. Dual-hysteron model of the GMI bi-hysteretic behavior, which can be decomposed into a hysteron (blue)/anti-hysteron (red) pair. It represents the irreversible switches of the μ_t. (For interpretation of the references to color in this figure legend, the reader is referred to the web version of this article.)

$H^+_\downarrow$ transition. We defined the combination of coupled hysteron and anti-hysteron as dual-hysteron (Fig. 5). It is characterized by a unique saturation level of lower μ_t, $\mu_{\downarrow,}$ and each of them is associated with the μ_t behavior of one local structure in the ribbon. In summary, a dual-hysteron describes a complex hysteretic operator where the necessary applied field to provoke an up transition depends on the sign of the last saturation reached, while the return to lower μ_t state is not influenced by the applied magnetic field past history. It is composed of a pair of hysteron/anti-hysteron linked together through the higher μ_t state. It is noteworthy to remember that dual-hysteron is a construction based on the observation of the GMI major curve and the GMI–FORCs' paths, in order to adequately analyze FORC distribution from even functions. The FORC distribution itself remains distribution of mathematical hysterons.

4.3. FORC distribution

The real (R) and imaginary (X) parts of the GMI signal present similar FORC distributions, calculated with Eqs. (1) and (2) respectively. Both mainly exhibits two features which may be directly associated to the hysteron/anti-hysteron pair (Fig. 6). As predicted, a positive peak (A), corresponding to the hysteron, appears in the low H_r region, while a negative one (B), resulting from the anti-hysteron path, is located in the second region. The position of the peaks can be considered as the average transition fields between the μ_t states (see Fig. 5 for R-related values), while their broad distribution indicates a gradual transition of the local structures. It is worth noticing that this information can not be obtained from the major GMI spectra, because it is related to physical processes occurring locally in the soft magnetic ribbon. Finally, despite the global GMI spectra symmetry, one can observe that the dual-hysteron components are of similar width (≈ 2.7 Oe) but non-symmetrically located (≈ -1.5 vs ≈ 0.7 Oe).

In addition of these characteristical features, the FORC distributions exhibit another positive peak (C), which is more apparent in the real part diagram (Fig. 6(b), approximately located at $H=-H_r=2.1$ Oe). Its position may suggest the possibility of symmetric hysterons, i.e. μ_t transitions that occur for identical applied field amplitude, whatever the sweep field direction.

4.4. Parameters influence

In all cases, decreasing the ac current frequency ($f=200$–500 kHz) decreases the $H_\uparrow$ values of both dual-hysteron components (H position of peak A (Fig. 7) and H_r of peak B for respectively the hysteron and anti-hysteron). This dependence could arise from

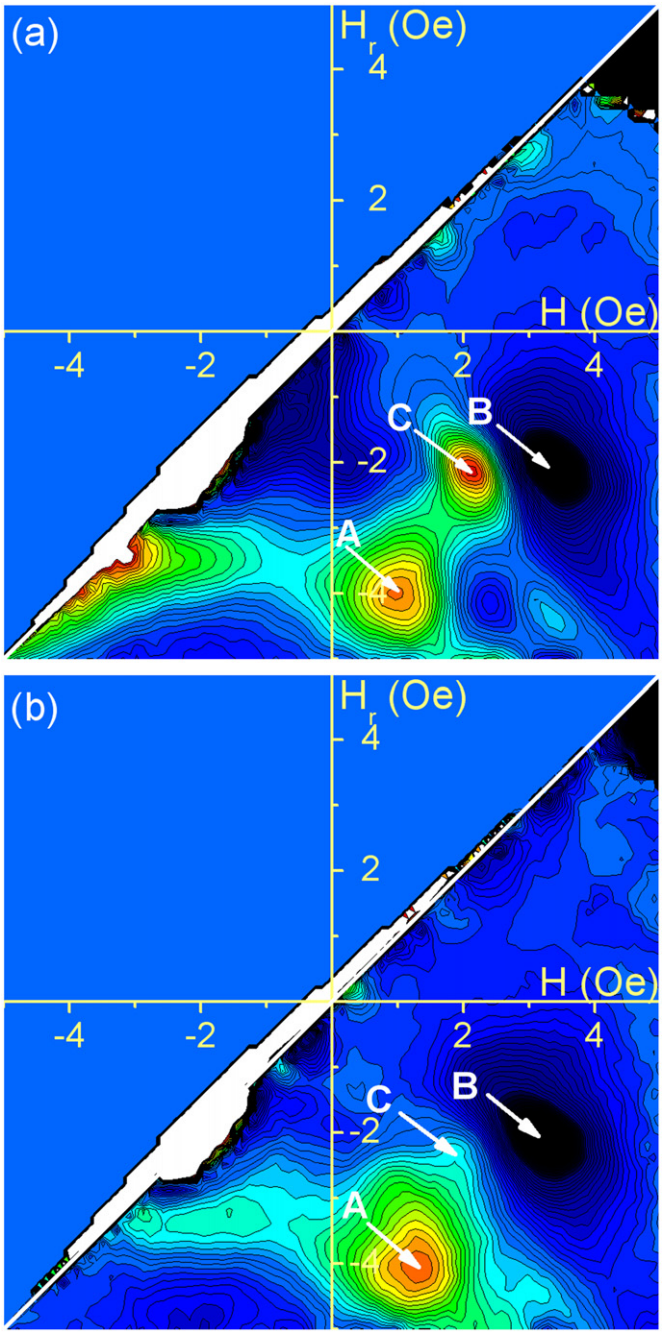

Fig. 6. Typical FORC diagram from the (a) real part and (b) imaginary part of the GMI signal of an amorphous ribbon. The positive part ranges from pale blue ($\rho=0$) to red (maximum value of ρ), while blue goes darker as the ρ value decreases in the negative part. It is noteworthy that the experimental data cover only the lower triangle of the contour plot, because no data are taken for $H<H_r$. (For interpretation of the references to color in this figure legend, the reader is referred to the web version of this article.)

volume non-homogeneity of the local structures changing μ_t. Furthermore, we observed an increasing trend of their width $H_c=(H-H_r)/2$ with the anisotropy constant K, indicating that the transversal anisotropy hardens the irreversible μ_t switching (Fig. 7).

5. Conclusion

In conclusion, we have applied the FORC formalism to study the hysteretic behavior of GMI effect. We propose a dual-hysteron

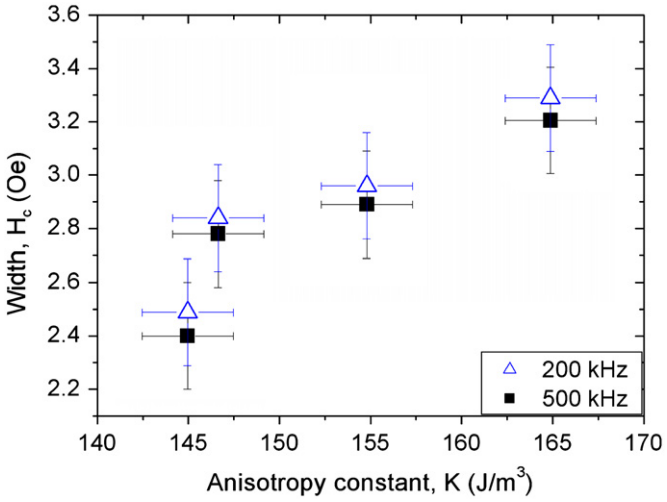

Fig. 7. Hysteron width $H_c=(H-H_r)/2$ in function of the anisotropy.

model, which successfully matches the resulting FORC distribution. This method now gives us the tools to adequately investigate this GMI peculiarity, which is important for both fundamental magnetic studies and technological applications. The approach presented here opens the possibility for further studies concerning the FORC analysis applied to different hysteretic systems through magneto-transport phenomena.

Acknowledgments

This work was financially supported in part by the Brazilian agencies FAPESP, FAPEMIG, CAPES and CNPq and Canadian agency FQRNT. J. M. Barandiaran is acknowledged for supplying the samples. A. Yelon and D. Ménard are also acknowledged for fruitful ideas and discussions regarding GMI in novel magnetic materials.

References

[1] E.P. Harrison, G.L. Turney, H. Rowe, H. Gollop, Proceedings of the Royal Society of London 157 (1937) 651.
[2] F.L.A. Machado, C.S. Martins, S.M. Rezende, Physical Review B 51 (1995) 3926.
[3] K.R. Pirota, L. Kraus, M. Knobel, P.G. Pagliuso, C. Rettori, Physical Review B 60 (1999) 6685.
[4] L.V. Panina, K. Mohri, T. Ushiyama, M. Noda, K. Bushida, IEEE Transactions on Magnetics. 31 (1995) 1249.
[5] L. Kraus., Journal of Magnetism and Magnetic Materials 195 (1999) 764.
[6] D. Ménard, A. Yelon, Journal of Applied Physics 88 (2000) 379.
[7] P. Ciureanu, L.G.C. Melo, D. Seddaoui, D. Menard, A. Yelon, Journal of Applied Physics 72 (2007) 073908.
[8] R.L. Sommer, C.L. Chien, Applied Physics Letters 67 (1995) 857.
[9] J.P. Sinnecker, P. Tiberto, G.V. Kurlyandskaia, E.H.C.P. Sinnecker, M. Vázquez, A. Hernando, Journal of Applied Physics 84 (1998) 5814.
[10] M. Vázquez, G.V. Kurlyandskaia, J.M. Garcia-Beneytez, J.P. Sinnecker, J.M. Barandiarán, V.A. Lukshina, A.P. Potapov, IEEE Transactions on Magnetics 35 (1999) 3358.
[11] M. Tejedor, B. Hernando, M.L. Sánchez, V.M. Prida, G.V. Kurlyandskaya, D. García, M. Vázquez, Journal of Magnetism and Magnetic Materials 215–216 (2000) 425.
[12] D. García, G.V. Kurlyandskaya, M. Vázquez, F.I. Toth, L.K. Varga, Journal of Magnetism and Magnetic Materials 203 (1999) 208.
[13] D. Ménard, D. Frankland, P. Ciureanu, A. Yelon, M. Rouabhi, R.W. Cochrane, H. Chiriac, T.A. Óvári, Journal of Applied Physics 83 (1998) 6566.
[14] M. Knobel, M. Vázquez, L. Kraus, in: K.H.J. Buschow (Ed.), Handbook of Magnetic Materials 15, Elsevier, London, 2003, p. 497.
[15] I.D. Mayergoyz, Physical Review Letters 56 (1986) 1518.
[16] H.G. Katzgraber, F. Pázmándi, C.R. Pike, K. Liu, R.T. Scalettar, K.L. Verosub, G.T. Zimányi, Physical Review Letters 89 (2002) 257202.
[17] F. Béron, L. Clime, M. Ciureanu, D. Ménard, R.W. Cochrane, A. Yelon, Journal of Nanoscience and Nanotechnology 8 (2008) 2944;
K. Seal, S. Jesse, M.P. Nikiforov, S.V. Kalinin, I. Fujii, P. Bintachitt, S. Trolier-McKinstry, Physical Review Letters 103 (2009) 057601.
[18] J. Wong, P. Greene, R.K. Dumas, K. Liu, Applied Physics Letters 94 (2009) 032504.
[19] J.-G. Ramírez, A. Sharoni, Y. Dubi, M.E. Gómez, I.K. Schuller, Physical Review B 79 (2009) 235110.
[20] M. Fecioru-Morariu, D. Ricinschi, P. Postolache, C.E. Ciomaga, A. Stancu, L. Mitoseriu, Journal Optical Advanced Materials 6 (2004) 1059.
[21] R. Tanasa, A. Stancu, E. Codjovi, J. Linares, F. Varret, J.-F. Letard, Journal of Applied Physics 103 (2008) 07B905.
[22] J.M. Pomeroy, T.C. White, H. Grube, J.C. Read, J.E. Davies, Applied Physics Letters 95 (2009) 022514.
[23] K.R. Pirota, M.L. Sartorelli, M. Knobel, J. Gutierrez, J.M. Barandiarán, Journal of Magnetism and Magnetic Materials 202 (1999) 431.
[24] F. Béron, G. Soares, M. Knobel, K.R. Pirota, Review of Scientific Instruments 82 (2011) 063904.
[25] F. Béron, D. Ménard, A. Yelon, Journal of Applied Physics 103 (2008) 07D908.